

# On the Mechanism of Pinning in Phase-Separating Polymer Blends

Claudio Castellano\* and Sharon C. Glotzer†

*Center for Theoretical and Computational Materials Science, and Polymers Division, National  
Institute of Standards and Technology, Gaithersburg, MD 20899*

(October 26, 2018)

## Abstract

We re-explore the kinetics of spinodal decomposition in off-critical polymer blends through numerical simulations of the Cahn-Hilliard equation with the Flory-Huggins-De Gennes free energy functional. Even in the absence of thermal noise, the solution of the discretized equation of motion shows coarsening in the late stages of spinodal decomposition without evidence of pinning, regardless of the relative concentration of the blend components. This suggests this free energy functional is not sufficient to describe the physics responsible for pinning in real blends.

---

\*Permanent address: Dipartimento di Scienze Fisiche, Università degli studi di Napoli, Pad. 19, Mostra d'Oltremare, Napoli 80125, Italy. Internet address: castellano@na.infn.it

†Internet address: glotzer@ctcms.nist.gov

## I. INTRODUCTION

Experiments on spinodal decomposition in polymer blends show that the coarsening process may sometimes slow dramatically or even cease before reaching equilibrium [1] - [6]. In these systems, spinodal decomposition — which is the process by which a thermodynamically unstable mixture demixes to a stable, phase-separated equilibrium state [7] - [13] — proceeds normally for some time following a quench to the unstable region ( $T < T_s$ ), and then stops. A break-up of the characteristic, interconnected pattern is observed to precede this pinning phenomenon. The nonequilibrium, microphase-separated blend has been observed to remain in this pinned state over an appreciable time scale where little domain growth occurs. The eventual breakup of the evolving morphology into separated droplets is a natural consequence of the asymmetric composition in an off-critical blend [14]; nevertheless, it may also occur in near-critical blends due to other forces (e.g. gravity). Polymer blends in which pinning has recently been observed for off-critical composition include X-7G/poly(ethylene terephthalate) (a liquid crystalline polymer/homopolymer blend) [1], poly(styrene-*ran*-butadiene)/polybutadiene [4], poly(styrene-*ran*-butadiene)/polyisoprene [4], and polybutadiene/polyisoprene [6].

The specific mechanism responsible for pinning in these blends is poorly understood, and is currently a topic of considerable discussion. While there is general agreement that growth stops soon after the breakup into separated “droplets” or “clusters” (a so-called “percolation-to-cluster transition” [4,14]), the mechanism that prevents further coarsening of disconnected domains remains to be clarified. One intriguing scenario points to an entropic barrier as the reason for the observed arrested growth of off-critical phase separating blends. Kotnis and Muthukumar (KM) [15] have suggested that due to the connectivity of the chains and the reduced conformational entropy near domain interfaces [16], the usual evaporation-condensation mechanism of coarsening [17] observed in small-molecule mixtures is suppressed in polymer blends, and instead coarsening occurs via parallel transport of chains along the interface [18]. Consequently, KM postulate that if the concentration of the minority-rich

phase becomes smaller than the percolation threshold, the parallel coarsening mechanism will be inhibited and the clusters will “freeze” after an initial growth period.

Hashimoto and coworkers have instead postulated that the enthalpy of mixing, rather than the entropy, provides the barrier to further coarsening following the percolation-to-cluster transition [4]. They argue that the increase in enthalpy of mixing suffered upon removing a chain of species  $A$  and degree of polymerization  $N$  from the surface of an  $A$ -rich domain is  $\Delta H_{\text{mix}} \propto \chi N k_B T$ , where  $\chi$  is the Flory interaction parameter,  $k_B$  is Boltzmann’s constant, and  $T$  is temperature. In the strong segregation limit  $\chi N \gg 1$ , and thus evaporation of the chain from the domain surface, which would occur with a Boltzmann probability proportional to  $\exp(-\Delta H_{\text{mix}}/k_B T)$ , is highly unfavorable. Thus, when the parallel transport mechanism is eliminated by the breakup into droplets, coarsening ceases.

In this paper, we re-explore the kinetics of spinodal decomposition in off-critical polymer blends described by the Flory-Huggins-De Gennes (FHDG) free energy functional, through numerical simulations of the Cahn-Hilliard (CH) equation. In Sec. II, we discuss the CH-FHDG equation and the origin of the concentration-dependent square gradient coefficient that has been proposed by KM to cause pinning in off-critical blends. The discretization and numerical integration scheme used to solve this equation, and our numerical results, are presented in Sec. III and discussed in Sec. IV. Finally, a summary of our main conclusions, and speculations on possible mechanisms of pinning in blends, is discussed in Sec. V.

## II. THEORETICAL MODEL

Model blends are typically described by the Flory-Huggins-De Gennes free energy functional [19–21]:

$$\frac{F\{\phi(\mathbf{r})\}}{k_B T} = \int d^3r \left[ \frac{f_{FH}(\phi(\mathbf{r}))}{k_B T} + \kappa(\phi)(\nabla\phi)^2 \right], \quad (2.1)$$

with

$$\kappa(\phi) = \frac{\sigma_a^2}{36\phi} + \frac{\sigma_b^2}{36(1-\phi)} + \chi\lambda^2, \quad (2.2)$$

where  $\phi(\mathbf{r})$  is the local concentration of component  $A$  (so that  $1-\phi$  is the concentration of component  $B$ ),  $\sigma_A$  and  $\sigma_B$  are the Kuhn lengths of the two species,  $\lambda$  is an effective interaction distance between monomers, and the Flory-Huggins free energy is [22,23]

$$\frac{f_{FH}(\phi)}{k_B T} = \frac{\phi}{N_A} \ln \phi + \frac{(1-\phi)}{N_B} \ln(1-\phi) + \chi\phi(1-\phi), \quad (2.3)$$

where  $N_A$  ( $N_B$ ) is the degree of polymerization of chains  $A$  ( $B$ ). Whereas in small molecule mixtures the square gradient coefficient is enthalpic (arising from short range interactions between molecules) and independent of the local concentration [24], De Gennes proposed that the connectivity of polymer molecules in inhomogeneous blends manifests itself through an additional, concentration-dependent contribution to the square gradient coefficient  $\kappa(\phi)$  [19]. The expression for  $\kappa(\phi)$  in Eq. 2.2 was derived to be consistent with the random phase approximation result for the inverse structure factor of an incompressible polymer blend [21,25,26],

$$S^{-1}(\mathbf{q}) = \frac{1}{N_A \phi_o D(q^2 R_A^2)} + \frac{1}{N_B (1-\phi_o) D(q^2 R_B^2)} - 2\chi. \quad (2.4)$$

Here  $R_i^2$  is the average square radius of gyration of species  $i$ ,  $\phi_o$  is the average value of the concentration and the Debye function is  $D(x) = 2[x - 1 + e^{-x}]/x^2$ , with  $x \equiv q^2 R_i^2$ . In the weak segregation limit, the interfacial width is much larger than the chain dimensions [24], so that the length scales of interest are larger than  $R_i$  ( $q^2 R_i^2 \ll 1$ ), and thus the Debye function may be approximated by  $D^{-1}(x) = 1 + x/3 + O(x^2)$ . The square gradient coefficient in Eq. 2.2 is then obtained from the coefficient of the  $q^2$  term in the Taylor expansion of the inverse structure factor, which is related to the free energy functional by [21]  $S^{-1}(\mathbf{q}) = (k_B T)^{-1} \delta^2 F / \delta \phi^2$ , where the r.h.s. is evaluated in  $q$ -space.

Because of the approximations made in the calculation of the square gradient expression, the Flory-Huggins-de Gennes free energy functional describes the physics of blends in the weak segregation limit, and on length scales much larger than the average chain dimension [12,24,27]. In strongly-segregating blends ( $\chi N \gg 1$ ) for which  $\chi$  is small but  $N \rightarrow \infty$ , Eq. 2.2 with a different prefactor in the  $\phi$ -dependent part is typically used [27-29].

The local part of the free energy (Eq. 2.3) has the same Ginzburg-Landau type of double-well structure as small molecules or Ising-like systems [30]. Thus, the only difference between the free energy functionals for the simplest small molecule and polymeric systems arises from the chain connectivity, which is expressed in the FHDG functional through the reduction of the entropic part of the local term, and by the  $\phi$ -dependent part of the square-gradient coefficient. KM proposed that the entropic contribution to the nonlocal part of the free energy, namely the concentration-dependent square-gradient coefficient, provides the barrier to coarsening which, when combined with the percolation-to-cluster transition, causes pinning of the off-critical phase-separating blend. In the next section, we re-examine the numerical solution of the time evolution of the CH-FHDG equation for both critical and off-critical blends. Specifically, we show that for this model pinning is *not observed* in the continuum limit, regardless of the blend composition, although a dynamical exponent slightly smaller than  $1/3$  is found.

The theoretical description of spinodal decomposition in binary blends is based on the Cahn-Hilliard-Cook equation for the time evolution of the concentration, originally derived for small molecule systems [7,31]:

$$\frac{\partial\phi}{\partial t} = \nabla \cdot \left( M(\phi) \nabla \frac{\delta F\{\phi\}}{\delta\phi} \right) + \eta(\mathbf{r}, t). \quad (2.5)$$

In this equation,  $M(\phi)$  is the mobility,  $F\{\phi\}$  is the coarse-grained free energy functional, and  $\eta$  is thermal noise. For polymers, the free energy functional is typically taken to be of the Flory-Huggins-De Gennes form in Eq. 2.1, but more general free energy functionals may be included.

In the following, we will always consider for simplicity a symmetric blend, for which  $N_A = N_B \equiv N$  and  $\sigma_A = \sigma_B \equiv \sigma$ . In this case, the mobility

$$M(\phi) = ND\phi(1 - \phi) \quad (2.6)$$

has been proposed [19], where  $D$  is the self-diffusion coefficient. We will also take the effective interaction distance  $\lambda$  equal to the Kuhn length  $\sigma$ . Substituting in Eq. 2.5 the functional

derivative of  $F$  and the expression for  $M$ , the time evolution of the concentration is given by:

$$\frac{\partial\phi(\mathbf{r},t)}{\partial t} = ND\nabla\left\{\phi(1-\phi)\nabla\left[\frac{1}{N}\ln\frac{\phi}{1-\phi} + \chi(1-2\phi) - \left(2\chi\sigma^2 + \frac{\sigma^2}{18\phi(1-\phi)}\right)\nabla^2\phi + \frac{(1-2\phi)\sigma^2}{36\phi^2(1-\phi)^2}(\nabla\phi)^2\right]\right\}. \quad (2.7)$$

Note that in Eq. 2.7 we have neglected the thermal noise term. Since we are interested in the presence or absence of pinning due to the FHDG free energy functional alone, and since it has been shown that the presence of thermal noise in the analogue of this equation for small molecule systems does not influence the scaling function or the growth exponent during coarsening [10,32], we will neglect noise in our simulations [33,34].

Eq. 2.7 can be rescaled so that it depends on dimensionless space and time variables. The transformation, valid only in the unstable region, is the following [15]:

$$\mathbf{x} = \frac{(\chi - \chi_s)^{1/2}}{\sigma}\mathbf{r} \quad \tau = \frac{D(\chi - \chi_s)^2}{\sigma^2\chi_s}t, \quad (2.8)$$

where  $\chi_s = 1/(2N\phi_0(1 - \phi_0))$  gives the spinodal curve and  $\phi_0$  is the average value of concentration. (This rescaling differs from the rescaling commonly used in experiments by a simple numerical factor.) After this transformation, Eq. 2.7 becomes [15]:

$$\frac{\partial\phi(\mathbf{x},\tau)}{\partial\tau} = \frac{1}{2\phi_0(1-\phi_0)}\nabla\left\{\phi(1-\phi)\nabla\left[\frac{\chi_c}{2(\chi-\chi_s)}\ln\frac{\phi}{1-\phi} - 2\frac{\chi}{\chi-\chi_s}\phi - \left(2\chi\sigma^2 + \frac{\sigma^2}{18\phi(1-\phi)}\right)\nabla^2\phi + \frac{(1-2\phi)\sigma^2}{36\phi^2(1-\phi)^2}(\nabla\phi)^2\right]\right\}. \quad (2.9)$$

### III. NUMERICAL SOLUTION

The solution of this continuum equation ( 2.9, which was first studied by KM [15], describes the time evolution of the concentration field after a quench to  $\chi > \chi_s$  in the unstable region [33,34]. The initial condition before the quench, corresponding to high temperature, is given by a uniform field with random fluctuations about its average value

$\phi_0$ . At early times following the quench, the uniform concentration is unstable with respect to the long wavelength fluctuations arising from the initial condition, and the two components begin to spatially separate. Domains rich in one or the other component form, and then coarsen so as to remove interfaces and minimize the free energy. In small-molecule mixtures described by, e.g., the Ginzburg-Landau free energy functional, these domains coarsen until phase separation is complete regardless of the relative composition and the presence of thermal noise. Our goal in this paper is to determine if the same is true for the FHDG free energy functional [34].

In the late stages of decomposition, the system can be characterized by the evolution of the typical size of growing domains. The scaling hypothesis [35] states that this length  $L$  (as calculated from, e.g., the inverse of the peak position of the structure factor, the inverse of the first moment of the structure factor, the position of the first zero in the pair correlation function, etc.) evolves in time according to

$$L \sim \tau^\alpha. \quad (3.1)$$

The choice of one particular definition of  $L$  is dictated only by convenience. Numerical simulations, experiments, and analytical results strongly support the validity of the scaling hypothesis in small molecule systems, giving in the absence of hydrodynamic forces the value  $\alpha = 1/3$  independent of quench depth, relative composition, and the presence of noise [10]. While polymers are believed to belong to the same static universality class as small molecules, the situation is less clear with respect to dynamics.

To study the kinetics of spinodal decomposition in polymer blends, we numerically integrate Eq. 2.9 via a finite difference scheme for both time and space variables. The continuous space of position vectors is replaced by  $n^3$  sites on a simple cubic lattice with mesh size (lattice spacing)  $\Delta x$ . The temporal discretization is achieved by replacing the continuous time variable  $\tau$  by a series of  $m$  discrete time steps of duration  $\Delta\tau$ . The value of the concentration field at all sites at each time step is then computed by a first-order Euler numerical integration scheme [36], described in detail in the Appendix.

Although a large time step and mesh size would speed up the computation, the mesh size must be chosen carefully so as to be smaller than the smallest important length scale in the problem at all times — here the interfacial width, which decreases in time until the latest stages of demixing. The size of the time step is in turn limited by the mesh size. A time step that is too large could generate instabilities and spurious solutions [32,36]. Thus, these discrete variables must be chosen carefully in concert. A linear stability analysis can be helpful in suggesting reasonable trial values. If the algorithm is stable with these values of  $\Delta x$  and  $\Delta\tau$ , one can then vary them to find optimum values and to ensure that the solution is accurate and *independent* of the choice of these parameters.

We have studied the effect on the numerical solution of Eq. 2.9 of changing  $\Delta x$ ;  $\Delta\tau$  is changed suitably so as to maintain stability. The boundary conditions are periodic in all three directions. Initial conditions are given by random values of the concentration field, with average  $\phi_0$  and a flat distribution between  $\phi_0 - \Delta\phi_0$  and  $\phi_0 + \Delta\phi_0$ .  $\Delta\phi_0$  has a strong influence on the behavior during the initial regime, but does not affect the late stage behavior. Therefore we fix  $\Delta\phi_0 = 0.1$ . Several realizations of the initial conditions were averaged together for every set of parameters.

The phase separation is monitored visually in real space, and quantitatively by determining the time evolution of  $k_1(\tau)$ , the first moment of the spherically-averaged structure factor [13]; this is the inverse length that is used to determine the exponent  $\alpha$ . For the purposes of comparison with previous studies [15,34], we take  $\chi$  to be related to  $T$  (K) by [37]:

$$\chi = 0.326/T - 2.3 \cdot 10^{-4}, \quad (3.2)$$

and fix  $T_c = 62$  °C. The system was quenched to temperatures  $T = 54.5, 49$  and  $25$  °C for critical composition ( $\phi_o = 0.5$ ), and to temperatures  $T = 35$  and  $15$  °C for off-critical composition ( $\phi_o = 0.4$ ).

We first consider the solution of Eq. 2.9 obtained with a mesh size  $\Delta x = 1$ , time step  $\Delta\tau = 0.01$  and  $n = 32$  (Fig. 1). This choice of mesh size gives, e.g. for  $T = 35$  °C and



$\phi_0 = 0.4$ , an equivalent dimensional mesh size of  $\Delta r \approx 6R_g$ , where  $R_g$  is the average chain radius of gyration. With these choices, we are exactly repeating the integration of Eq. 2.9 previously performed by Kotnis and Muthukumar. Our results reproduce their findings. For critical quenches ( $\phi_0 = 0.5$ ), after an initial transient, the system enters the late stage regime, where  $k_1$  decays in time with a power law. The exponent  $\alpha$  appears to be smaller than  $1/3$ , the value expected for spinodal decomposition in small molecule systems and for polymer blends in the intermediate stages of demixing (ie. without hydrodynamics). For off-critical quenches ( $\phi_0 = 0.4$ ), domain growth stops before the phase separation is complete.

Results change drastically when the mesh size is reduced to  $\Delta x = 0.5$ , for which the time step must be reduced to  $\Delta\tau = 0.002$  to maintain numerical stability (Fig. 2). (Note that in this case we must take  $n = 64$  to keep the system size the same as before —  $n \cdot \Delta x = 32$ ). This choice of mesh size gives, e.g. for  $T = 35^\circ\text{C}$  and  $\phi_0 = 0.4$ , an equivalent dimensional mesh size of  $\Delta r \approx 3R_g$ . In this case, the late stage behavior is the same for both critical and off-critical quenches, even after the blend undergoes the percolation-to-cluster transition. After an initial transient, the late stage scaling regime is reached:  $k_1$  decays as a power law and no pinning is observed. The values of  $\alpha$  can be computed from the slopes of the curves in Fig. 2 and are reported in Table I. In all cases  $\alpha$  is found to be greater than  $1/4$  and smaller than  $1/3$ . We believe that the latter is the true asymptotic value for this free energy functional; the small systematic error may be attributed to the crossover from the preasymptotic regime and, possibly, to the numerical slowing down given by a still oversized mesh size (see Sec. IV). Increased accuracy might be obtained by using an even smaller value for  $\Delta x$ , but this implies a suitable reduction in the value of  $\Delta\tau$ , and as a result, a prohibitively large computation time.

The critical relevance of the mesh size to the late stage behavior of the system is also evident from Fig. 3, where a “pinned” state obtained with  $\Delta x = 1$  is “depinned” by reducing the mesh size to 0.5.

## IV. DISCUSSION

The absence of pinning for small mesh sizes in our simulations even for off-critical quenches clearly shows that what is observed for  $\Delta x = 1$  is not a physical effect but only an artifact of the discretization. By integrating Eq. 2.9 via a discretization scheme, we are actually changing the model under consideration: the solution of the discrete model exactly reproduces that of the continuum equation only in the limit where  $\Delta t$  and  $\Delta x$  approach zero. For this reason one must always confirm that the numerical results are independent of the values of the discretization variables. In particular, it was recently shown that an oversized mesh size can cause a non-physical freezing of interfacial motion for systems with non-conserved order parameter [38]. “Spurious pinning” was already noted by Rogers et al. [32] in a conserved order parameter system, who showed that for the Cahn-Hilliard equation with the Ginzburg-Landau free energy functional, a mesh size  $\Delta x > 1.7$  causes an unphysical decrease in the effective growth exponent.

In general, the solution of the discrete model should reproduce the behavior of the continuum equation if  $\Delta x$  is much less than the smallest physical length modeled in the system. In the case under investigation, we are studying a polymer blend in the weak segregation limit ( $\chi \geq \chi_c, \chi \ll 1$ ). The smallest physical length that must be resolved is the interfacial width, which during the late stages of phase separation is of the order of the correlation length  $\xi$  [24]:

$$\xi \sim \frac{R_g}{(\chi - \chi_c)^{1/2} \cdot N^{1/2}} \sim \frac{\sigma}{(\chi - \chi_c)^{1/2}}, \quad (4.1)$$

which is close to unity in rescaled units. Choosing  $\Delta x = 1$  implies that we are resolving the system at a length *equal* to the correlation length. The spatial derivatives at the interfaces are consequently computed inaccurately with this mesh size, thereby producing unphysical results. This picture is confirmed by Fig. 4 showing that when  $\Delta x = 1$  the interface appears only one mesh size wide. When  $\Delta x = 0.5$  the interface is smoother, and larger than the mesh size; hence no pinning occurs. This effect also explains the low estimates of  $\alpha$  for

critical quenches when  $\Delta x = 1$  — the sharpness of the interface unphysically slows down the evolution of the solution, even if it is not sufficient to pin it. Possibly also the results for  $\Delta x = 0.5$  are slightly biased by this effect.

It is possible to understand the origin of this problem in another way by looking directly at the equation of motion. Consider for simplicity a one-dimensional small molecule system (i.e. the square-gradient coefficient  $\kappa$  and the mobility  $M$  are constant), where the concentration profile goes from one bulk value ( $\phi_1$ ) at site  $x_i - \Delta x$  to the other ( $\phi_2$ ) at site  $x_i + \Delta x$ , through an interface. For the domain size to grow, the interface must move, and thus  $\phi(x_i)$  must change from  $\phi_1$  to  $\phi_2$ . The driving force for this change is the square gradient term in the free energy, which yields a Laplacian in the functional derivative of  $F$ . This force must overcome the double well potential given by the local term in the free energy expression, as stated by the Cahn-Hilliard equation:

$$\frac{\partial \phi}{\partial t} = M \nabla^2 \left( \frac{\partial f}{\partial \phi} - \kappa \nabla^2 \phi \right). \quad (4.2)$$

In the discrete version of this equation, the local part does not depend on  $\Delta x$ , while the Laplacian is given by:

$$\nabla^2 \phi = \frac{1}{(\Delta x)^2} [\phi(x_i + \Delta x) + \phi(x_i - \Delta x) - 2\phi(x_i)]. \quad (4.3)$$

When we increase  $\Delta x$  the denominator grows indefinitely, while the numerator is bounded above by  $\phi_2 + \phi_1 - 2\phi(x_i) = \text{const.}$  Then, increasing  $\Delta x$  *decreases* the value of the Laplacian term, while the local term is unchanged. For  $\Delta x$  large enough the Laplacian cannot overcome the local term, the solution stops evolving, and the system artificially “pins”.

## V. CONCLUSION

In summary, we have shown that both critical and off-critical polymer blends described by the Flory-Huggins-De Gennes free energy functional undergo spinodal decomposition via the Cahn-Hilliard equation without pinning of the domain growth as observed in some

experiments. Even in the absence of thermal noise [34], the solution of the discretized equation of motion shows coarsening without evidence of pinning, regardless of the relative concentration of the blend components. We have also shown that previous solutions of the CH-FHDG equation that exhibited pinning were artifacts of an oversized mesh size used in the discretization and numerical integration of the equation of motion, and *not* a result of the concentration-dependence of the square gradient coefficient as previously suggested [15]. This suggests the FHDG free energy functional alone, as written in Eq. 2.1 is not sufficient to describe the physics responsible for pinning in real blends.

Evidently, a model able to describe the arrested growth observed in experiments must include additional physical ingredients. One should consider that experimental blends which exhibit pinning often contain components which are not simple homopolymers; such is the case with Hashimoto's random copolymer/homopolymer blends, as well as with Hasegawa's liquid-crystalline polymer/homopolymer blend, in which the liquid-crystalline component is anisotropic at the quench temperatures at which pinning was observed. These blends may not be describable by the simple Flory-Huggins-De Gennes expression, and consequently we should not expect the CH-FHDG equation to mimic their behavior during spinodal decomposition. It is also important to note that a significant fraction of homopolymer blends never exhibit pinning, regardless of the relative composition. However, for those that do, it is possible that either the mobility, or free energy functional, or both, must be appropriately modified. The simplified expression for mobility (Eq. 2.6) used in the CH-FHDG equation, which was originally derived only for the special case of a perfectly symmetric blend [19], may neglect important contributions to mobility arising from the connectivity within the polymer chains.

With respect to possible free energy modifications, it is well known that interfacial growth can be slowed or stopped by decreasing the interfacial tension. This can be achieved by, e.g. using surfactants in the case of small molecules [39], diblock copolymers in the case of polymers [40], or impurities in the case of alloys [41]. If the experimental blends contain even a small number of impurities, or specific interaction regions that act as impurities

[42], these impurities could arrest the demixing process and cause pinning. Finally, the FHDG free energy functional in Eq. 2.1 describes incompressible blends; real blends are in fact compressible. A coupling of concentration fluctuations and density fluctuations may be responsible for pinning in blends [43], in which case a reformulation of the free energy functional as well as the addition of a second order parameter field is necessary.

We are extremely grateful to J. Douglas, B. Hammouda, P. Gallagher, C. Han, E. Di-Marzio, G. McFadden, A. Coniglio, F. Corberi and J. Warren, and especially to M. Muthukumar, A. Chakrabarti and G. Brown, for useful discussions. We thank the Center for Computational Science at Boston University and the University of Maryland for generous use of their CM-5. CC would like to thank the Structure and Mechanics Group in the Polymers Division at NIST, and the NIST Center for Theoretical and Computational Materials Science, for their hospitality.

## VI. APPENDIX

The numerical solution of Eq. 2.9 is performed via iteration of the following map:

$$\phi_{i,j,k}^{m+1} = \phi_{i,j,k}^m + \Delta\tau \frac{\partial \phi_{i,j,k}^m}{\partial \tau}. \quad (6.1)$$

This map, given the value of the concentration field  $\phi_{i,j,k}^m$  at time  $m\Delta\tau$  at each of the  $n^3$  sites of a simple cubic lattice with mesh size  $\Delta x$ , yields the value of  $\phi_{i,j,k}^{m+1}$  at each site at time  $(m+1)\Delta\tau$ . Note that the mesh size is taken to be the same in all directions.

The time derivative  $\partial \phi_{i,j,k}^m / \partial \tau$  is given by the discretization of the left hand side of Eq. 2.9, with spatial derivatives centrally discretized. This means the chemical potential  $\mu_{i,j,k}^m$  that appears in square brackets in Eq. 2.9 is computed using:

$$[\nabla \phi(\mathbf{x}, \tau)]^2 \rightarrow \left( \frac{\phi_{i+1,j,k}^m - \phi_{i-1,j,k}^m}{2\Delta x} \right)^2 + \left( \frac{\phi_{i,j+1,k}^m - \phi_{i,j-1,k}^m}{2\Delta x} \right)^2 + \left( \frac{\phi_{i,j,k+1}^m - \phi_{i,j,k-1}^m}{2\Delta x} \right)^2, \quad (6.2)$$

and

$$\nabla^2 \phi(\mathbf{x}, \tau) \rightarrow \frac{\phi_{i+1,j,k}^m - 2\phi_{i,j,k}^m + \phi_{i-1,j,k}^m}{(\Delta x)^2} + \frac{\phi_{i,j+1,k}^m - 2\phi_{i,j,k}^m + \phi_{i,j-1,k}^m}{(\Delta x)^2} +$$

$$\frac{\phi_{i,j,k+1}^m - 2\phi_{i,j,k}^m + \phi_{i,j,k-1}^m}{(\Delta x)^2}. \quad (6.3)$$

The divergence of the product  $\phi(1 - \phi)\nabla\mu$  is evaluated as follows:

$$\begin{aligned} \nabla \cdot \{\phi(1 - \phi)\nabla\mu\} \rightarrow & \left( \frac{X_{i+1,j,k}^m - X_{i-1,j,k}^m}{2\Delta x} \right) + \left( \frac{Y_{i,j+1,k}^m - Y_{i,j-1,k}^m}{2\Delta x} \right) + \\ & \left( \frac{Z_{i,j,k+1}^m - Z_{i,j,k-1}^m}{2\Delta x} \right), \end{aligned} \quad (6.4)$$

where

$$X_{i,j,k}^m = \left( \frac{\mu_{i+1,j,k}^m - \mu_{i-1,j,k}^m}{2\Delta x} \right) (\phi_{i,j,k}^m (1 - \phi_{i,j,k}^m)), \quad (6.5)$$

and  $Y_{i,j,k}^m$  and  $Z_{i,j,k}^m$  are defined accordingly.

## REFERENCES

- [1] H. Hasegawa, T. Shiwaku, A. Nakai and T. Hashimoto, in *Dynamics of Ordering Processes in Condensed Matter*, edited by S. Komura and H. Furukawa (Plenum, New York, 1988).
- [2] T. Hashimoto, in *Dynamics of Ordering Processes in Condensed Matter*, edited by S. Komura and H. Furukawa (Plenum, New York, 1988).
- [3] A. Wong and P. Wiltzius (unpublished).
- [4] T. Hashimoto, M. Takenaka, and T. Izumitani, *J. Chem. Phys.* **97**, 679 (1992); M. Takenaka, T. Izumitani and T. Hashimoto, *J. Chem. Phys.* **98**, 3528 (1993).
- [5] T. Hashimoto in *Material Science and Technology: Phase Transformations in Materials* **12**, edited by P. Haasen (Weinham: VCH, 1993), 251.
- [6] J. Lauger, R. Lay, and W. Gronski, *J. Chem. Phys.* **101**, 7181 (1994).
- [7] J.W. Cahn and J.E. Hilliard, *J. Chem. Phys.* **28**, 258 (1958); J.W. Cahn, *Acta Metall.* **9**, 795 (1961); *Acta Metall.* **10**, 179 (1962); *J. Applied Phys.* **34**, 3581 (1963); General Electric Research Lab. Report, RL3561M (1964); *Acta Metall.* **14**, 1685 (1966); *Trans. Metall. Soc. AIME* **242**, 166 (1968).
- [8] J.D. Gunton, M. San Miguel and P.S. Sahni, in *Phase Transitions and Critical Phenomena* **8**, edited by C. Domb and J. L. Lebowitz (Academic Press, London, 1983).
- [9] T. Hashimoto, *Phase Transitions* **12**, 47 (1988).
- [10] K. Binder in *Material Science and Technology: Phase Transformations in Materials* **5**, edited by P. Haasen (Weinham: VCH, 1990), pp. 405-471.
- [11] C.C. Han and A.Z. Akcasu, *Ann. Rev. Phys. Chem.* **43**, 61 (1992).
- [12] K. Binder, *Adv. in Poly. Sci.* **112**, 181 (1994).

- [13] S.C. Glotzer in *Annual Reviews of Computational Physics*, **II**, 1, D. Stauffer, ed. (World Scientific, Singapore, 1995).
- [14] S. Hayward, D.W. Heermann, and K. Binder, *J. Stat. Phys.* **49**, 1053 (1987).
- [15] M. Kotnis and M. Muthukumar, *Macromolecules* **25**, 1716 (1992).
- [16] E. Helfand and Y. Tagami, *J. Chem. Phys.* **56**, 3592 (1972); E. Helfand and A.M. Sapse, *J. Chem. Phys.* **62**, 1327 (1975); E. Helfand, *Macromolecules* **9**, 307 (1976).
- [17] I.M. Lifshitz and V.V. Slyozov, *J. Phys. Chem., Solids* **19**, 35 (1961).
- [18] D.A. Huse, *Phys. Rev. B* **34**, 7845 (1986).
- [19] P.G. De Gennes, *J. Phys.(Paris) Lett.* **38L**, 441 (1977). P.G. De Gennes, *J. Chem. Phys.* **72**, 4756 (1980).
- [20] P. Pincus, *J. Chem. Phys.* **75**, 1996 (1981).
- [21] K. Binder, *J. Chem. Phys.* **79**, 6387 (1983).
- [22] P.J. Flory, *J. Chem. Phys.* **9**, 660 (1941); *Principles of Polymer Chemistry*, Cornell University Press, Ithaca, 1953.
- [23] M.L. Huggins, *J. Chem. Phys.* **9**, 440 (1941).
- [24] For a nice discussion, see G. Fredrickson in *Physics of Polymer Surfaces and Interfaces*, edited by I.C. Sanchez, (Butterworth-Heinemann, Boston, 1992).
- [25] S.F. Edwards, *Proc. Phys. Soc.* **88**, 265 (1966).
- [26] A.Z. Akcasu and M. Tombakoglu, *Macromolecules* **23**, 607 (1989); A.Z. Akcasu, R. Klein, and B. Hammouda, *Macromolecules* **26**, 4136 (1993).
- [27] H. Tang and K.F. Freed, *J. Chem. Phys.* **94**, 1572 (1991); H. Tang and K.F. Freed, *J. Chem. Phys.* **94**, 6307 (1991); X.C. Zeng, D.W. Oxtoby, H. Tang, and K.F. Freed, *J. Chem. Phys.* **96**, 4816 (1992).



- [28] R.J. Roe, *Macromolecules* **19**, 728 (1986).
- [29] W. McMullen, in *Physics of Polymer Surfaces and Interfaces*, edited by I.C. Sanchez, (Butterworth-Heinemann, Boston, 1992).
- [30] N. Goldenfeld, *Lectures on Phase Transitions and the Renormalization Group*, Addison-Wesley Publication Co., MA, 1992.
- [31] H.E. Cook, *Acta Metall.* **18**, 297 (1970).
- [32] T.M. Rogers, K.R. Elder and R.C. Desai, *Phys. Rev. B* **37**, 9638 (1988), and references therein.
- [33] Eq. 2.7 with concentration-independent mobility and thermal noise was first studied for critical quenches in A. Chakrabarti, R. Toral, J.D. Gunton and M. Muthukumar, *Phys. Rev. Lett.* **63**, 2072 (1989); A. Chakrabarti, R. Toral, J.D. Gunton and M. Muthukumar, *J. Chem. Phys.* **92**, 6899 (1990); J.D. Gunton, R. Toral and A. Chakrabarti, *Physica Scripta T* **33**, 12 (1990). Solutions of that equation and the CH-GL equation were compared for critical quenches in A. Chakrabarti and G. Brown, *Phys. Rev. A* **46**, 981 (1992).
- [34] Eq. 2.7 with concentration-independent mobility and thermal noise was studied for off-critical quenches in G. Brown and A. Chakrabarti, *J. Chem. Phys.* **98**, 2451 (1993). No pinning was observed in their simulations.
- [35] K. Binder and D. Stauffer, *Phys. Rev. Lett.* **33**, 1006 (1974).
- [36] W.H. Press, B.P. Flannery, S.A. Teukolsky and W.T. Vetterling, *Numerical Recipes*, Cambridge University Press, Cambridge, 1990.
- [37] P. Wiltzius, F.S. Bates and W. Heffner, *Phys. Rev. Lett.* **60**, 1538 (1988); F.S. Bates and P. Wiltzius, *J. Chem. Phys.* **91**, 3258 (1989).
- [38] B. Merriman, J.K. Bence and S.J. Osher, *J. Comp. Phys.* **112**, 334 (1994).

- [39] Gompper and Schick, in *Phase Transitions and Critical Phenomena* **16**, Domb and Lebowitz, eds. 1994; M. Laradji, H. Guo, M. Grant, and M.J. Zuckermann, *J. Phys. A* **24**, L629 (1991); *J. Phys. Condens. Matter* **4**, 6715 (1992).
- [40] T. Hashimoto and T. Izumitani, *Macromolecules* **26**, 3631 (1992).
- [41] D.A. Huse and C.H. Henley, *Phys. Rev. Lett.* **54**, 2708 (1985); G. Grest and D.J. Srolovitz, *Phys. Rev. B* **32**, 3014 (1985); D.J. Srolovitz and G. Grest, *Phys. Rev. B* **32**, 3021 (1985); S. Puri, D. Chowdhury and N. Parekh, *J. Phys. A* **24**, L1087 (1991); S. Puri and N. Parekh, *J. Phys. A* **25**, 4127 (1992).
- [42] S.C. Glotzer, M.F. Gyure, F. Sciortino, A. Coniglio, and H.E. Stanley, *Phys. Rev. Lett.* **70**, 3275 (1993); *Phys. Rev. E* **49**, 247 (1994); F. Sciortino, P. Alstrom, R. Bansil, and H.E. Stanley, *Phys. Rev. E* **47**, 4615 (1993).
- [43] J.F. Douglas, private communication.

## FIGURES

FIG. 1. Plot of  $\log(k_1)$  vs  $\log(\tau)$  for a system with  $n = 32$  and  $\Delta x = 1$ . Each curve is the average over 5 realizations with different initial conditions.

FIG. 2. Plot of  $\log(k_1)$  vs  $\log(\tau)$  for a system with  $n = 64$  and  $\Delta x = 0.5$ . Each curve for critical quenches is the average over 5 realizations with different initial conditions. Each curve for off-critical quenches is averaged over 10 realizations.

FIG. 3. (a) Snapshot of a 2D slice of a system of size  $n = 32$  and  $\Delta x = 1$  at  $\tau = 100$ . (b) The same system for  $\tau = 200$ . (c) The same system in (a) at  $\tau = 200$  when  $\Delta x$  is switched to 0.5 at  $\tau = 100$ . The decrease of mesh size allows the system to phase-separate without pinning.

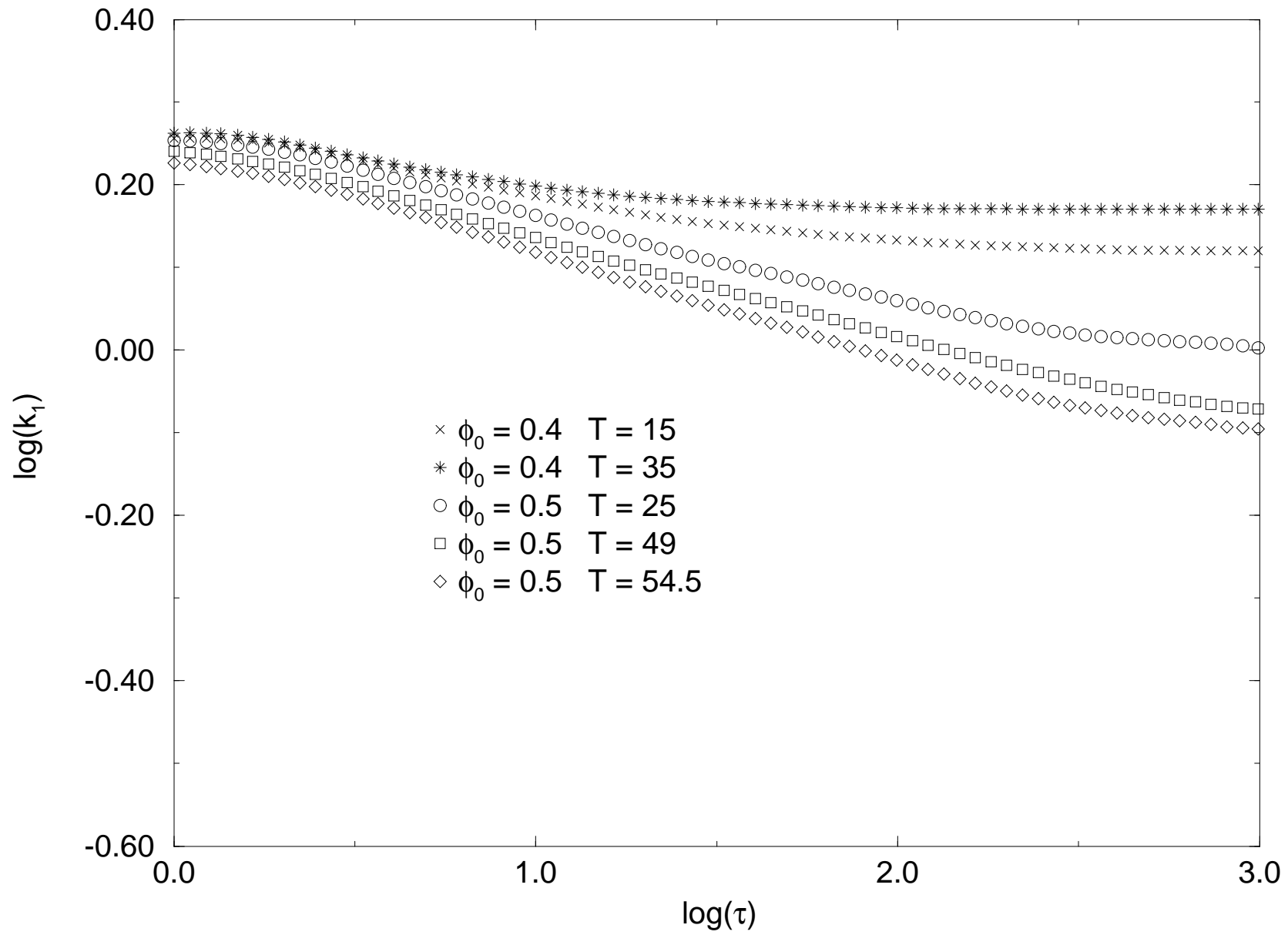
FIG. 4. Interface profile for (a)  $\Delta x = 1$  and (b)  $\Delta x = 0.5$ , for  $n = 32$ ,  $\phi_0 = 0.4$ ,  $T = 15$  and  $\tau = 100$ .

TABLES

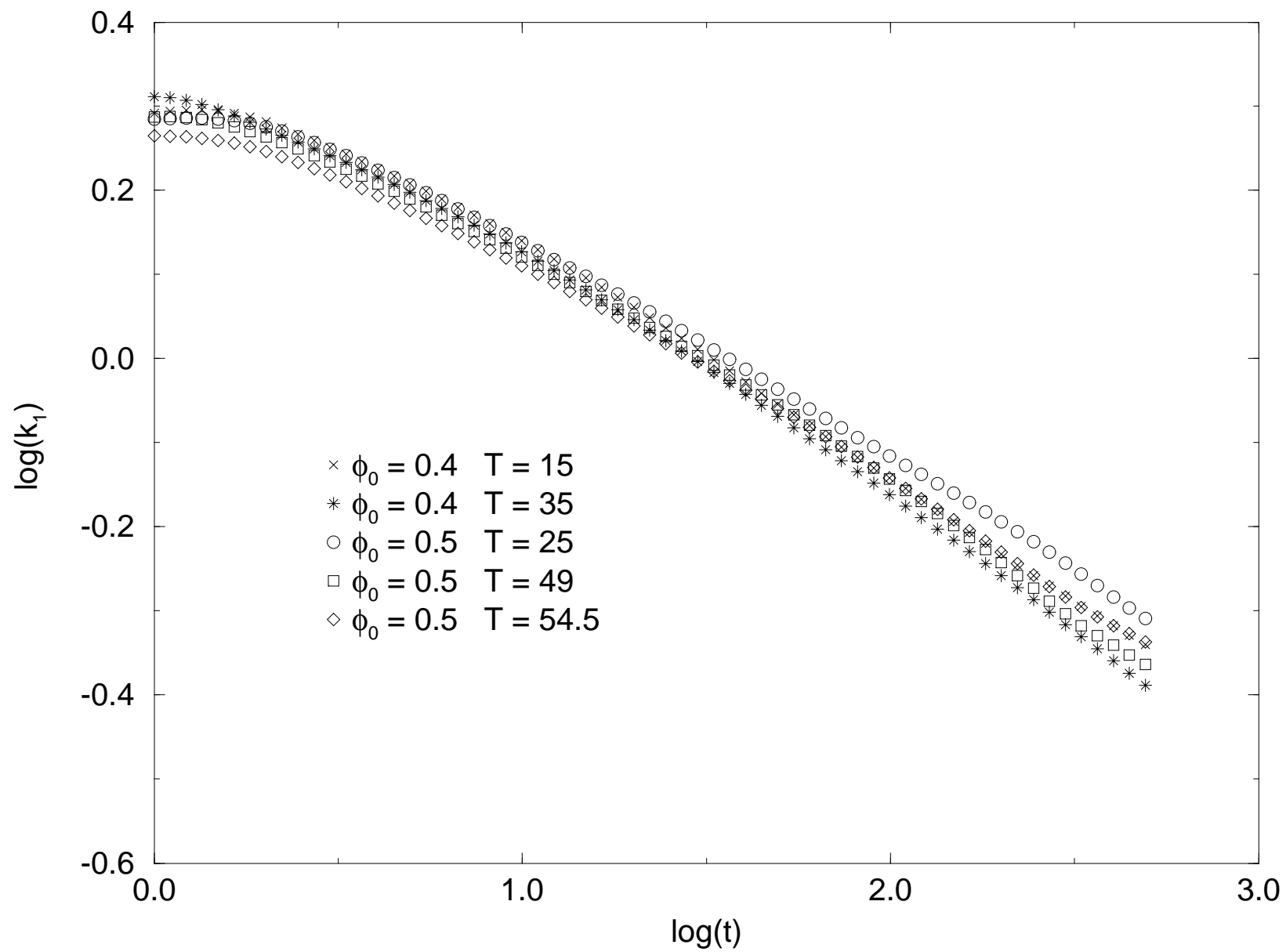
Critical quenches ( $\Delta\phi_o = 0.5$ )			
T	25	49	54.5
$\alpha$	$0.263 \pm 0.001$	$0.286 \pm 0.002$	$0.270 \pm 0.001$
Off-critical quenches ( $\Delta\phi_o = 0.4$ )			
T	15		35
$\alpha$	$0.290 \pm 0.001$		$0.306 \pm 0.001$

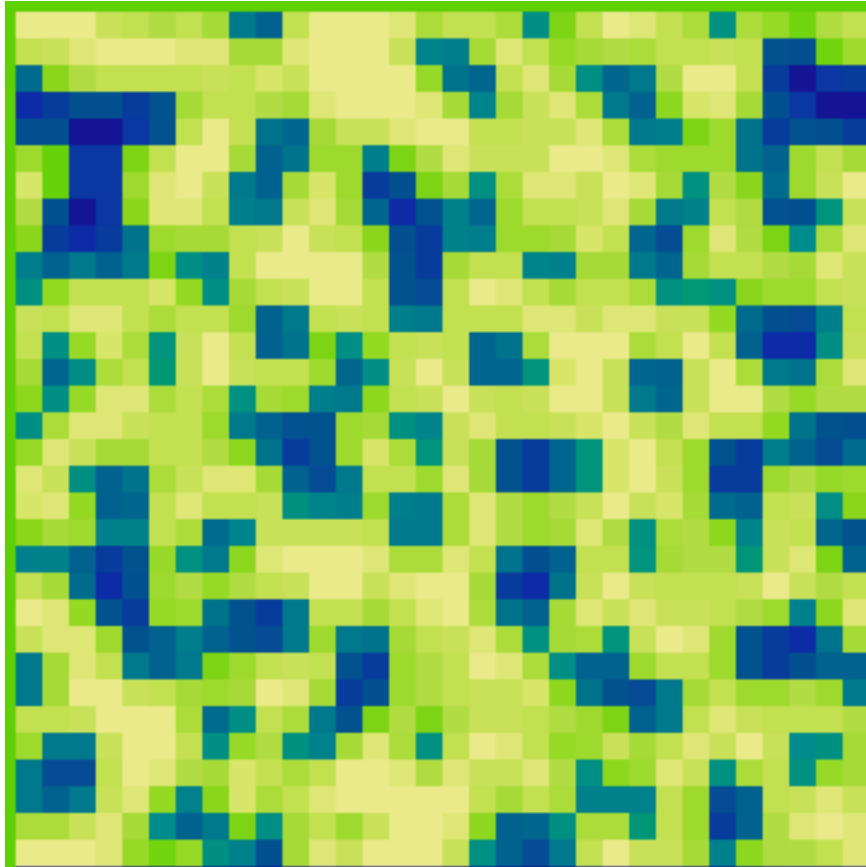
TABLE I. Values of the dynamic exponent  $\alpha$  for  $n = 64$  and  $\Delta x = 0.5$ , computed for  $\tau > 10$ . The exponents and errors were computed using a linear regression fit of the average values plotted in Fig. 2.

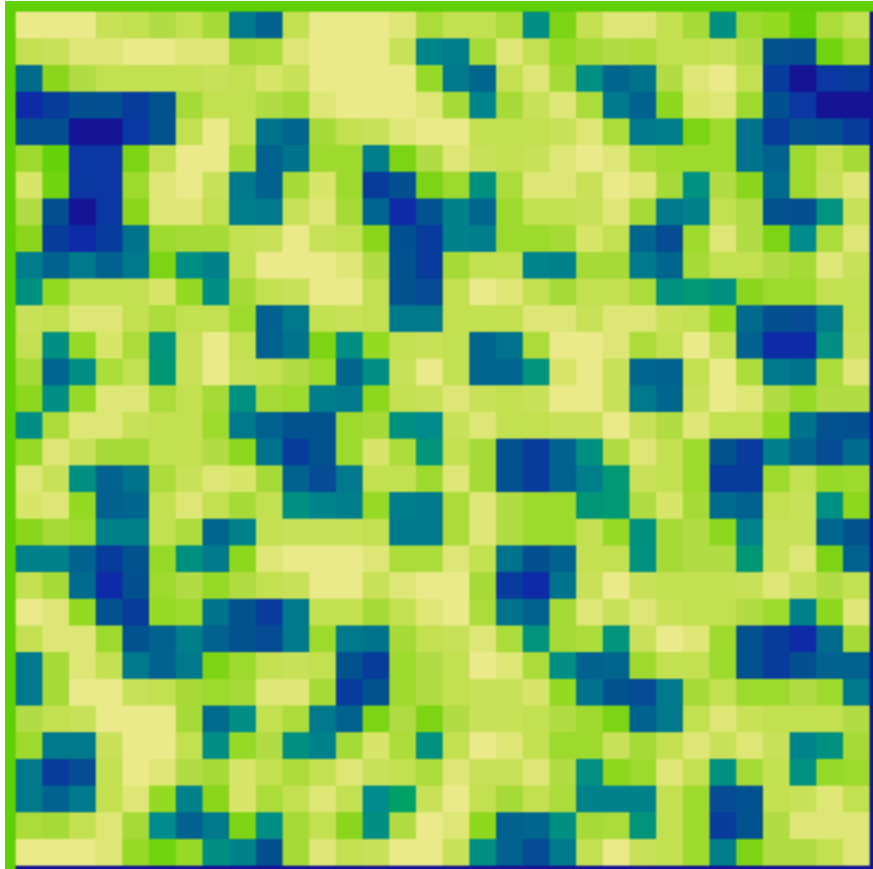
$n = 32 \quad \Delta x = 1$



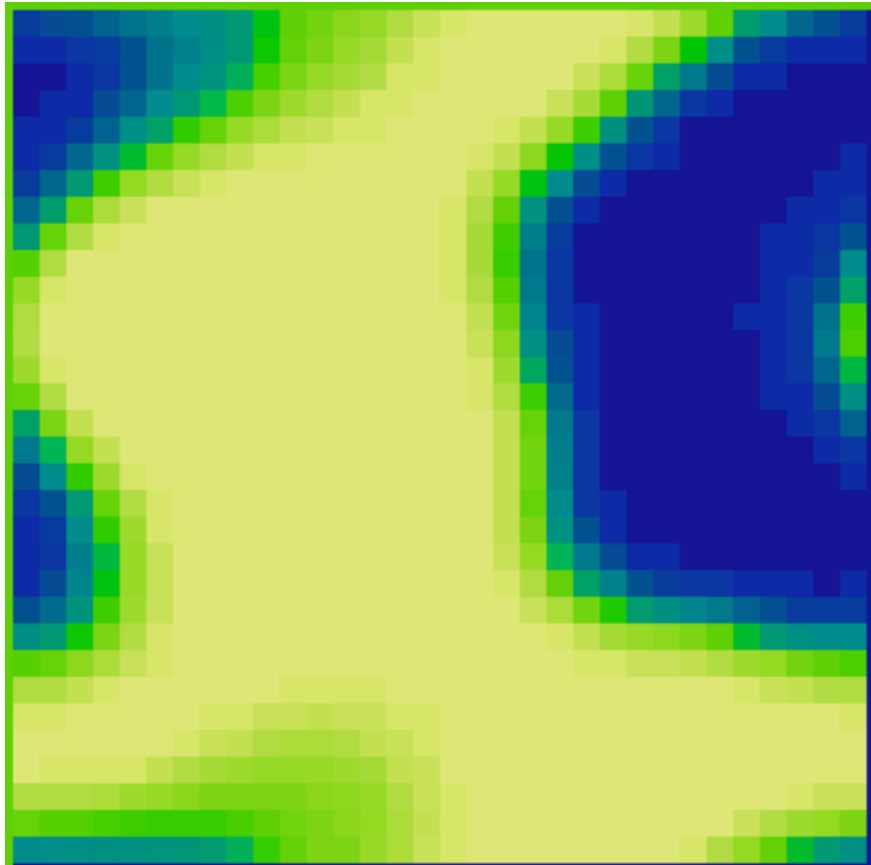
$n = 64 \quad \Delta x = 0.5$





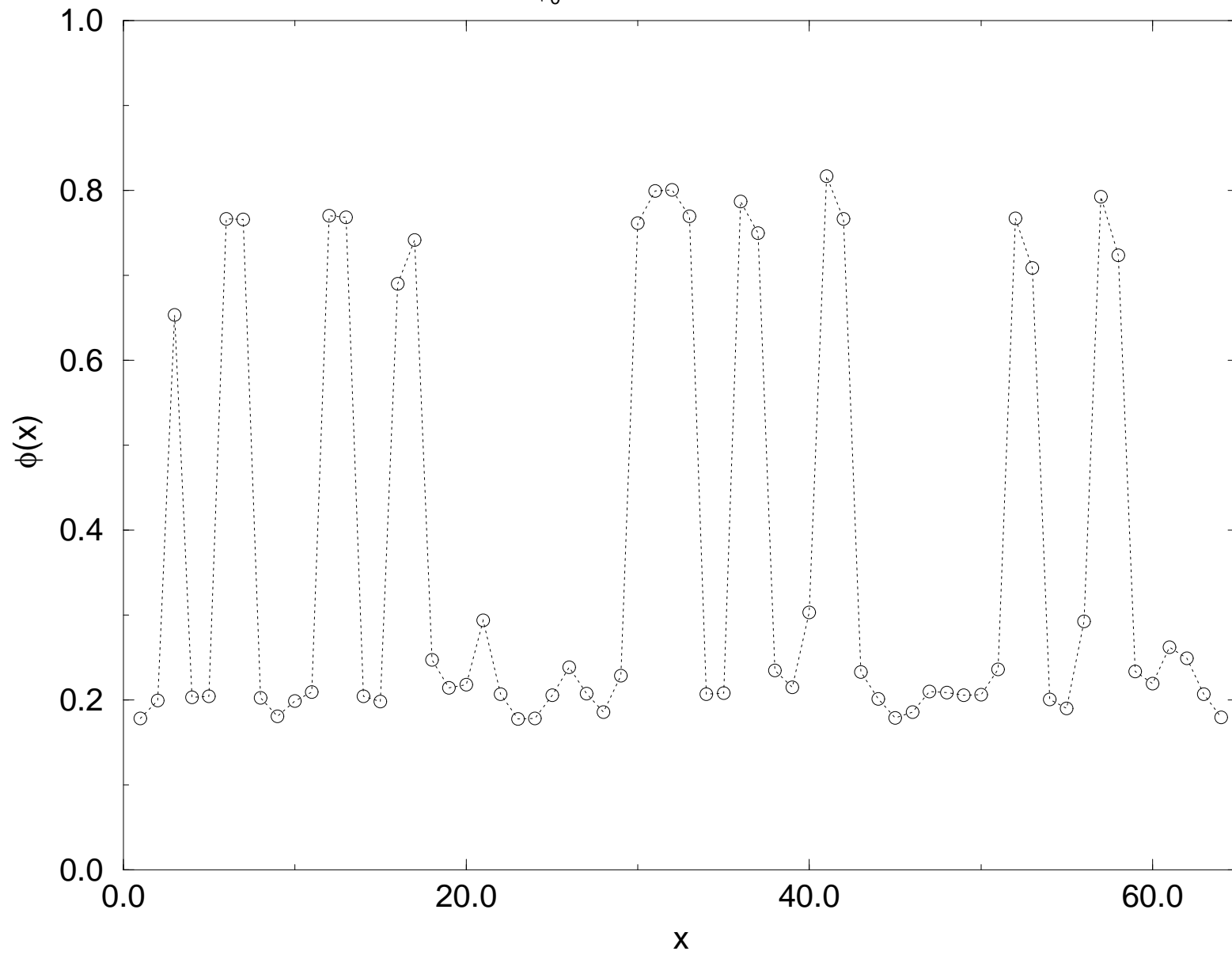






$n = 32 \quad \Delta x = 1$

$\phi_0 = 0.4 \quad T = 15 \quad t = 100$



$n = 64 \quad \Delta x = 0.5$

$\phi_0 = 0.4 \quad T = 15 \quad t = 100$

